Supplementary Information for:

Diminished Reward Responsiveness is Associated with Lower Reward Network GluCEST: An Ultra-High Field Glutamate Imaging Study

Valerie J. Sydnor, Bart Larsen, Christian Kohler, Andrew J. D. Crow, Sage L. Rush, Monica E. Calkins, Ruben C. Gur, Raquel E. Gur, Kosha Ruparel, Joseph W. Kable, Jami F. Young, Sanjeev Chawla, Mark A. Elliott, Russell T. Shinohara, Ravi Prakash Reddy Nanga, Ravinder Reddy, Daniel H. Wolf, Theodore D. Satterthwaite, David R. Roalf

Supplementary Figures

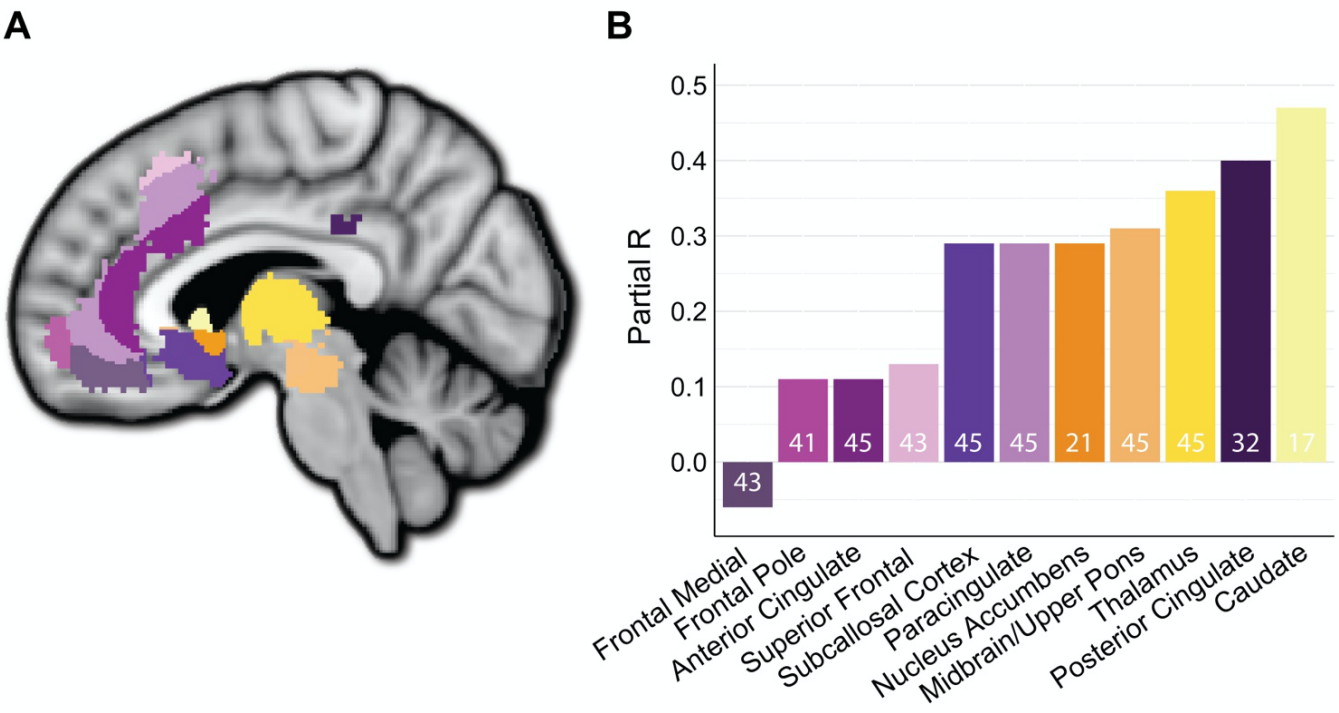

Supplementary Figure 1. Effect Size by Reward Network Anatomical Subdivision. A) The reward network segmented into 7 cortical (purple/pink) and 4 subcortical (yellow/orange) subregions. **B)** Effect sizes for the association between regional GluCEST contrast and BAS Reward Responsiveness scores across the 11 subregions. Minimum coverage of 50 mm^3 was required for inclusion in this regional analysis. The sample size for each region is indicated within the bar.

Supplementary Methods

Participant Recruitment, Study Exclusion Criteria, and Sample Medication Information

Participants were recruited from the community through ongoing research and clinical activities in the Brain Behavior Laboratory, the Lifespan Brain Institute, the Penn Psychosis Evaluation & Recovery Center, and the Outpatient Psychiatry Center at the Perelman School of Medicine, University of Pennsylvania. Study exclusion criteria included a previous or current significant medical or neurological illness, previous head trauma with loss of consciousness, acute intoxication, acute substance withdrawal, substance abuse or dependence within the past six months, pregnancy, contraindications to receiving an MRI, and GluCEST data that failed rigorous visual quality assurance checks. This study did not exclude individuals with a history of psychotropic medication use from the clinical group. Eighteen individuals in the clinical group reported a history of being prescribed at least one psychotropic medication, representing 40% of the entire sample and 60% of the clinical sample. Reported medications were highly variable across individuals, and included antidepressants (N=7), anxiolytics (N=1), mood stabilizers (N=3), antipsychotics (N=2), stimulants (N=4), and class not reported (N=5).

Additional Information on Clinical Questionnaires

All participants completed clinical questionnaires on the day of the MRI scan, with the exception of two participants who completed questionnaires 6 and 15 days prior to scanning.

Behavioral Activation System Scale: A Measure of Reward Responsiveness

The Behavioral Activation System (BAS) Scale comprises 13 questions answered on a 4-point Likert scale, and provides insight into motivational systems that influence an individual's affect and behavior [1]. The BAS Reward Responsiveness (BAS RR) subscale is a reliable measure of reward sensitivity that predicts happiness levels during reward anticipation [1], behavior on reward tasks [2–4], and brain responses to rewards [5, 6]. BAS RR scores have been found to remain stable over time despite fluctuations in clinical state [7].

The Patient-Reported Outcomes Measurement Information System Depression Scale

The Patient-Reported Outcomes Measurement Information System (PROMIS) Depression scale consists of 8 questions answered on a 5-point Likert scale. Questions assess feelings of sadness, helplessness, hopelessness, and worthlessness. To index overall depression severity, the eight PROMIS items were summed into a composite depression symptom severity score.

PRIME Screen-Revised

The PRIME Screen-Revised (PS-R) assesses the presence of positive psychotic symptoms, and is sensitive to both sub- and supra-threshold psychosis symptomatology. The 12 PS-R items, answered on a 7-point Likert scale, were summed into a composite score. Two participants did not have data for one PRIME item; the two missing values were imputed by taking the average of all other items.

Neuroimage Acquisition Parameters

GluCEST

Glutamate is an optimal metabolite to quantify with CEST imaging at 7.0T given that the proton exchange rate with water is slow to intermediate. This exchange regimen allows for continuous application of radiofrequency pulses and a prolonged saturation period, and thus for accumulation of the contrast effect and enhanced methodological sensitivity. The contrast effect is produced when exchangeable amine protons on glutamate that are saturated via frequency-selective radiofrequency pulses exchange with unsaturated protons on water, decreasing the bulk water signal. Hence, a higher concentration of tissue glutamate leads to increased B_1 saturation of glutamate protons, greater proton exchange and attenuation of the water signal, and a higher GluCEST contrast. The GluCEST contrast displays high within-day and between-day reproducibility [8]. Mathematically, the GluCEST contrast (%) is defined as:

$$\frac{\mathrm{Msat}(-3\mathrm{ppm}) - \mathrm{Msat}(+3\mathrm{ppm})}{\mathrm{Msat}(-3\mathrm{ppm})} \times 100$$

where Msat(-3ppm) is the amplitude of water proton magnetization during a baseline acquisition when glutamate protons are not saturated, and Msat(+3ppm) is the amplitude of water proton magnetization when the B_1 field is at the resonance frequency for glutamate (3 ppm downfield from water, see [9]).

GluCEST data were acquired in a right hemisphere sagittal slice in a field of view (FOV) placed near the midline. This FOV captures major reward network regions including the medial prefrontal cortex, posterior cingulate, ventral striatum, thalamus, and midbrain. Placement of the GluCEST FOV was initiated using ImScribe (https://www.med.upenn.edu/cmroi/imscribe.html). ImScribe was developed for use in group studies wherein acquisition of the same brain region(s) is desired, as it allows for reproducible selection of the same anatomical FOV across individuals.

The GluCEST acquisition parameters utilized in this study included: slice number = 1, slice thickness = 5 mm, FOV = 224 x 224, matrix size = 224 x 224, in-plane resolution = 1 x 1 mm^2, GRE read out TR = 6.4 ms, TE = 3 ms, number of averages = 1, shots per slice = 2, shotTR = 8000 ms. The CEST saturation pulse was as follows: B_{1rms} of 3.06 μT with a 800 ms long saturation pulse train consisting of a series of 95 ms Hanning windowed saturation pulses with a 5 ms interpulse delay (100 ms pulse train). Raw CEST images were acquired at varying saturation offset frequencies from ± 1.5 to ± 4.5 ppm (relative to water resonance) with a step size of ± 0.3 ppm. B_0 maps were acquired using water saturation shift referencing [10] with a saturation pulse at B_{1rms} of 0.29 μT with 200 ms long saturation pulse train and saturation offset frequencies from ± 0 to ± 1.5 ppm (relative to water resonance), with a step size of ± 0.15 ppm. A B_1 map was generated from three images obtained using square preparation pulses with flip angles 20°, 40°, and 80°. Total acquisition time was approximately 10 minutes.

MP2RAGE

Parameters for the 3D Magnetization Prepared 2 Rapid Acquisition Gradient Echoes (MP2RAGE) sequence were: 0.82 mm isotropic spatial resolution, 240 mm FOV with 176 slices, TR/TE/TI_1/TI_2/ = 5000/2.5/700/2500 ms, α_1/α_2 = 7°/5°, 240 Hz/Px bandwidth, 3 × GeneRalized Autocalibrating Partial

Parallel Acquisition (GRAPPA) acceleration in the first phase-encoding direction and 6/8 partial Fourier undersampling in both phase-encoding directions. With MP2RAGE acquisitions, data from short (INV1) and long (INV2) inversion time images can be combined to mitigate B_1 inhomogeneity effects. This produces a more homogeneous T1-weighted image with superior gray matter to white matter contrast, referred to as a uniform (UNI) image.

Reward Network Delineation

The meta-analytically derived reward network atlas [11] utilized in this study is comprised of brain regions that exhibited a significant change in the blood oxygen level-dependent (BOLD) signal in association with diverse rewarding outcomes and/or aversive outcomes across 206 functional MRI studies. The nature of outcomes was variable across these 206 studies and included monetary, social, consumable, and other outcomes. Hence, this network encompasses regions that evaluate or encode positively and negatively valenced outcomes across diverse situations and stimuli. Convergence across hundreds of functional MRI studies solidifies our confidence that these brain regions are central to reward responsiveness (RR).

The total meta-analytic functional reward network was divided into valence-related subcomponents for analyses presented in Figure 4. This was accomplished using valence maps from Bartra et al. (2013) Figure 3A-C [11]. The appetitive encoding component included voxels that exhibited an increase in BOLD signal to more rewarding outcomes only in the overall meta-analysis (Bartra et al. Figure 3A, excluding 3C). The aversive encoding component included voxels that exhibited an increase in BOLD signal to aversive or less rewarding outcomes only (Bartra et al. Figure 3B, excluding 3C). The salience component included voxels that exhibited an increase in BOLD signal to both rewarding and negative outcomes (Bartra et al. Figure 3C), and are thereby presumed to encode general reward salience.

Supplementary Results

GluCEST and Single Voxel ^{1}HMRS Demonstrate Cross-Method Agreement: Extended Methodology and Results

Single voxel of interest (VOI) ^{1}HMRS data were collected from the right anterior cingulate cortex in a subsample of study participants to enable a methodological comparison between ^{1}HMRS and GluCEST. ^{1}HMRS data were acquired at the end of the scanning session and were collected from participants only when adequate time permitted. The ^{1}HMRS VOI was positioned in the anterior cingulate to maximize comparability between the present study and the majority of previous investigations that assessed associations between RR and brain glutamate with ^{1}HMRS [12–16]. Below, we present findings from two sets of comparative analyses. In the first set of analyses, we studied the association between a) BAS RR scores and ^{1}HMRS glutamate concentration within the ^{1}HMRS VOI, and b) BAS RR scores and mean GluCEST contrast within this VOI. In the second set of analyses, we examined correlations between mean GluCEST contrast within the VOI and the concentration of numerous ^{1}HMRS-derived neurochemicals (including glutamate).

^{1}HMRS Acquisition, Neurometabolite Quantification, and Quality Control

The ^{1}HMRS VOI (average size 3000 mm^3) was placed using a semi-automated method via ImScribe; manual adjustment was used to fine-tune VOI positioning for each participant. ^{1}HMRS data were collected with a short echo time custom-modified Point RESolved Spectroscopy (PRESS) sequence with the following acquisition parameters: averages = 8 (water reference) / 128 (water suppressed), TE = 23 ms and TR = 3000 ms. Acquisition time was 36 seconds for the reference spectrum and 6 minutes 48 seconds for the suppressed spectrum. The water reference scan was used to compute the absolute concentration of brain neurochemicals, including absolute glutamate concentration. Water suppression was achieved with variable power RF pulses with optimized relaxation delays (VAPOR) prior to the acquisition. VAPOR implements seven frequency selective RF pulses to reduce sensitivity to variations in the B_1 field [17]. Pulse amplitudes were calibrated before measurement to reduce B_1 inhomogeneity

by acquiring six localized STimulated Echo Acquisition Mode (STEAM) water spectra at fixed reference voltage and varying flip angle from 0º to 180º with a step size of 30º. The vendor-provided FASTESTMAP shimming method (from vendor Siemens Medical Solutions, Erlangen, Germany) was employed to minimize spectral linewidths (< 30 Hz) of water signal [18]. Spectra obtained were analyzed using a user-independent spectral fit program, Linear Combination (LC) Model v6.3-1L with the corresponding 7T basis set [19]. To ensure that the ^{1}HMRS data used for comparative analyses was of high quality, participants with 1) a spectral peak full width half maximum (FWHM) > 0.1, 2) a signal-to-noise ratio (SNR) < 10, or 3) Cramer-Rao Lower Bound (CRLB) estimates > 15% for glutamate were excluded from all analyses. ^{1}HMRS data from 25 individuals passed these three ^{1}HMRS quality checks. From these 25 participants, an additional 5 participants were excluded from analyses due to low overlap between the ^{1}HMRS VOI and the GluCEST FOV (additional details below). Thus, 20 participants passed all quality control procedures.

Volume of Interest Processing and GluCEST Quantification

The ^{1}HMRS VOI was extracted from DICOM images and binarized to create a VOI mask using ImScribe. The cerebrospinal fluid volume fraction (fCSF) within the VOI mask was quantified for each participant (mean fCSF = 0.29 ± 0.12), as was the percent of the VOI occupied by reward network (mean percent = 55 ± 14) versus non-reward cortex (mean percent = 45 ± 14). To facilitate comparative analyses between ^{1}HMRS and GluCEST, the portion of the total VOI that was represented in each participant's 5 mm thick GluCEST FOV was extracted. This allowed for 1) quantification of the percent of the ^{1}HMRS VOI that overlapped with the GluCEST FOV, and 2) quantification of mean GluCEST, reward network GluCEST, and non-reward GluCEST within the portion of the ^{1}HMRS VOI included in the GluCEST FOV. For 5 of the 25 participants with ^{1}HMRS data that passed FWHM, SNR, and CRLB quality checks, the percent of the ^{1}HMRS VOI included in the GluCEST FOV was very low (< 20%). These 5 participants were thus excluded from analyses, given that methodological comparisons are not appropriate with such minimal anatomical overlap. GluCEST-^{1}HMRS comparative analyses were performed with the

remaining 20 participants (8 typically developing, 1 with a depressive disorder, 3 with a psychotic disorder, 8 clinical high risk). For each of these 20 participants, the percent of the ^{1}HMRS VOI included in the GluCEST FOV was > 45%.

Associations Between BAS RR Scores and Dual Method Anterior Cingulate Glutamate

^{1}HMRS-derived glutamate concentration and mean GluCEST contrast were quantified within the anterior cingulate cortex VOI, and entered as predictors of BAS RR scores in independent multiple linear regressions controlling for age, sex, and fCSF (^{1}HMRS model only). Replicating prior ^{1}HMRS studies of anterior cingulate glutamate and RR [12–16], neither the ^{1}HMRS-glutamate concentration (estimate = 0.15, $r_{PARTIAL}$ = 0.09, p = 0.733) nor the GluCEST contrast (estimate = 0.15, $r_{PARTIAL}$ = 0.06, p = 0.798) within the anterior cingulate VOI were associated with BAS RR scores. Harnessing the high-resolution image generated by the GluCEST acquisition, we were additionally able to parcellate the anterior cingulate VOI into reward and non-reward components, and to quantify mean GluCEST contrast within each component. Supporting this study's main findings, the association between BAS RR scores and mean GluCEST contrast was stronger in the reward network component of the anterior cingulate VOI ($r_{PARTIAL}$ = 0.27) than in the non-reward component of the VOI ($r_{PARTIAL}$ = 0.07). Taken together, this first set of comparative analyses reveals convergent findings across methods, underscores the importance of acquiring neurochemical imaging data from expansive FOVs, and highlights the benefit of function-based parcellation approaches.

GluCEST- and ^{1}HMRS-derived Measures of Brain Glutamate are Positively Correlated

Across the 20 participants included in this methodological comparison, on average 69% (± 23%) of the total ^{1}HMRS VOI was included in the GluCEST FOV. We were thus able to compare GluCEST and ^{1}HMRS measures within overlapping yet non-identical regions of the brain. Despite the fact that measures were derived from non-identical volumes of brain tissue with differing tissue fractions, there was a positive partial correlation (controlled for fCSF) between the GluCEST contrast and ^{1}HMRS-

derived glutamate concentration ($r_{PARTIAL}$ = 0.26, N = 20). As expected, the strength of this partial correlation was greater within participants who exhibited greater anatomical overlap between the ^{1}HMRS VOI and the GluCEST FOV. Specifically, the partial correlation between GluCEST and ^{1}HMRS glutamate increased in participants with > 50% anatomical overlap between ^{1}HMRS and GluCEST acquisitions ($r_{PARTIAL}$ = 0.36, N = 13), and further increased in those with > 90% anatomical overlap ($r_{PARTIAL}$ = 0.60, N = 5). Critically, the strength of the partial correlation between the GluCEST contrast and ^{1}HMRS neurochemical concentration was greater for glutamate than for other neurochemicals, including N-acetylaspartate ($r_{PARTIAL}$ = 0.02, N = 20), glutathione ($r_{PARTIAL}$ = -0.02, N = 17), and creatine/phosphocreatine ($r_{PARTIAL}$ = 0.14, N = 20). (All partial correlations were controlled for fCSF. Three participants were excluded from the glutathione analysis due to CRLB estimates > 15% for glutathione).

Diagnostic Group Differences in Regional GluCEST and Relationships to Prior 7.0T ^{1}HMRS Case-Control Studies

The primary goal of this study was to investigate dimensional associations between reward network glutamate level and inter-individual variability in RR across clinical diagnostic categories. However, we additionally capitalized on the inclusion of a diverse clinical population by examining differences in regional GluCEST between the typically developing group and each of the three clinical diagnostic groups (depressive disorders, psychotic disorders, and clinical high risk groups). One aim of these diagnostic group-based, regional analyses was to provide insight into the potential co-occurrence of neurochemical differences related to both a dimensional psychological construct and to patient diagnosis. A second, equally important aim was to assess whether diagnostic group-based differences obtained with GluCEST accord with the previously published 7.0T ^{1}HMRS case-control literature, offering a methodological validation.

Structural and functional MRI studies have implicated the anterior cingulate cortex [20–23] and the thalamus [20–22, 24, 25] in depressive and negative psychotic symptoms, in agreement with the role of these regions in the reward network. For this reason, prior single voxel 7.0T ^{1}HMRS studies investigating glutamatergic differences between a control group and patients with psychotic [26–36] or depressive [15, 32, 33, 37] disorders have most frequently chosen the anterior cingulate and the thalamus as cortical and subcortical ^{1}HMRS VOIs. As such, to embed the present diagnostic GluCEST data within the prior case-control ^{1}HMRS literature, we anatomically delineated the anterior cingulate cortex and thalamus with Harvard-Oxford atlases, quantified mean GluCEST contrast within these two regions, and examined group differences in regional GluCEST using ANCOVAs controlled for age and sex. ANCOVA results are presented below along with group mean z-scores, computed using control group means and standard deviations. Z-scores are provided to enable comparisons of standardized differences between the typically developing and diagnostic groups across regions and diagnostic categories.

GluCEST is Lower in Individuals Diagnosed with a Psychotic Disorder

Individual 7.0T ^{1}HMRS studies investigating glutamatergic differences between healthy controls and patients with psychotic disorders have produced rather heterogeneous results [38]. For example, prior work has reported either no significant difference in anterior cingulate cortex glutamate concentration between controls and patients [28, 31–35] or a lower concentration in patients [29, 36]. A recent meta-analysis of pooled data (9 studies, 255 patients, 293 controls) from these 7.0T studies, however, found evidence for an overall reduction in brain glutamate levels in psychosis [29]. In the present study, the GluCEST contrast was numerically lower in individuals with psychotic disorders (N=7) than in typically developing individuals (N=15) in both the anterior cingulate cortex and the thalamus. This difference was not significant in the anterior cingulate cortex (typically developing group mean z-score = 0 hereon, psychotic disorders group mean z-score = -0.43, $F_{1,18}$ = 0.59, p = 0.452) but was nearly significant in the thalamus (psychotic disorders group mean z-score = -1.45, $F_{1,18}$ = 4.36, p = 0.051). The present

GluCEST-derived results thus converge with the 7.0T ^{1}HMRS meta-analysis, as well as with a prior study of GluCEST in psychosis [39].

GluCEST is Not Significantly Different in Depression

To date, four 7.0T ^{1}HMRS studies have examined differences in anterior cingulate cortex [15, 32, 33, 37] and/or thalamic [33, 37] glutamate concentrations between healthy individuals and those with depression, and all have reported null results. Moreover, a large ^{1}HMRS meta-analysis of all available 1.5, 3.0, 4.0, and 7.0T studies additionally found no significant difference in anterior cingulate/medial prefrontal glutamate concentration between 371 patients with depression and 359 controls [40]. In accordance with these prior ^{1}HMRS results, we observed no significant difference in GluCEST contrast between typically developing (N=15) and depressive disorder (N=11) groups in either the anterior cingulate cortex (depressive disorders group mean z-score = 0.44, $F_{1,22}$ = 0.88, p = 0.358) or the thalamus (depressive disorders group mean z-score = -0.22, $F_{1,22}$ = 1.61, p = 0.218).

Clinical High Risk Individuals Tend to Have Higher GluCEST Than Those with Psychotic Disorders

To our knowledge, there are currently no published 7.0T ^{1}HMRS studies of individuals at clinical high risk for psychosis. However, a meta-analysis of lower field strength ^{1}HMRS studies did find significantly higher Glx (glutamate + glutamine) concentrations within the anterior cingulate/medial prefrontal cortex in high risk individuals compared to controls, but no significant group differences within the thalamus [41]. GluCEST data collected from those at clinical high risk for psychosis (N=12) for the current study again mirrored this pattern of previous findings (anterior cingulate cortex: clinical high risk group mean z-score = 0.39, $F_{1,23}$ = 1.31, p = 0.265; thalamus: clinical high risk group mean z-score = -0.02, $F_{1,23}$ = 0.086, p = 0.772). Notably, the GluCEST contrast was higher in individuals at clinical high risk for psychosis than in those with a diagnosed psychotic disorder in both the anterior cingulate cortex and the thalamus.

Altogether, these regional analyses of specific diagnostic groups align well with the extant 7.0T ^{1}HMRS literature. Furthermore, the results underscore the possibility that reward sensitivity and patient diagnosis may be differentially associated with glutamate availability in distinct brain areas. Nevertheless, given the small sample size of each clinical diagnostic group and known neurobiological heterogeneity within diagnostic categories [42], these diagnostic group-based GluCEST analyses must be considered preliminary.

Supplementary References

1. Carver CS, White TL. Behavioral inhibition, behavioral activation, and affective responses to impending reward and punishment: The BIS/BAS Scales. J Pers Soc Psychol. 1994;67:319–333.
2. Capa RL, Bouquet CA. Individual differences in reward sensitivity modulate the distinctive effects of conscious and unconscious rewards on executive performance. Front Psychol. 2018;9:148.
3. Suhr JA, Tsanadis J. Affect and personality correlates of the Iowa Gambling Task. Personal Individ Differ. 2007;43:27–36.
4. Braem S, Verguts T, Roggeman C, Notebaert W. Reward modulates adaptations to conflict. Cognition. 2012;125:324–332.
5. Van den Berg I, Franken IHA, Muris P. Individual differences in sensitivity to reward: Association with electrophysiological response to monetary gains and losses. J Psychophysiol. 2011;25:81–86.
6. Kim SH, Yoon H, Kim H, Hamann S. Individual differences in sensitivity to reward and punishment and neural activity during reward and avoidance learning. Soc Cogn Affect Neurosci. 2015;10:1219–1227.
7. Kasch KL, Rottenberg J, Arnow BA, Gotlib IH. Behavioral activation and inhibition systems and the severity and course of depression. J Abnorm Psychol. 2002;111:589–597.
8. Nanga RPR, DeBrosse C, Kumar D, Roalf D, McGeehan B, D'Aquilla K, et al. Reproducibility of 2D GluCEST in healthy human volunteers at 7 T. Magn Reson Med. 2018;80:2033–2039.
9. Cai K, Haris M, Singh A, Kogan F, Greenberg JH, Hariharan H, et al. Magnetic resonance imaging of glutamate. Nat Med. 2012;18:302–306.
10. Kim M, Gillen J, Landman BA, Zhou J, van Zijl PCM. Water saturation shift referencing (WASSR) for chemical exchange saturation transfer (CEST) experiments. Magn Reson Med. 2009;61:1441–1450.
11. Bartra O, McGuire JT, Kable JW. The valuation system: a coordinate-based meta-analysis of BOLD fMRI experiments examining neural correlates of subjective value. NeuroImage. 2013;76:412–427.
12. Colic L, von Düring F, Denzel D, Demenescu LR, Lord AR, Martens L, et al. Rostral anterior cingulate glutamine/glutamate disbalance in major depressive disorder depends on symptom severity. Biol Psychiatry Cogn Neurosci Neuroimaging. 2019;4:1049–1058.
13. Walter M, Henning A, Grimm S, Schulte RF, Beck J, Dydak U, et al. The relationship between aberrant neuronal activation in the pregenual anterior cingulate, altered glutamatergic metabolism, and anhedonia in major depression. Arch Gen Psychiatry. 2009;66:478–486.
14. Gabbay V, Mao X, Klein RG, Ely BA, Babb JS, Panzer AM, et al. Anterior cingulate cortex γ-aminobutyric acid in depressed adolescents. Arch Gen Psychiatry. 2012;69:139–149.
15. Godlewska BR, Masaki C, Sharpley AL, Cowen PJ, Emir UE. Brain glutamate in medication-free depressed patients: a proton MRS study at 7 Tesla. Psychol Med. 2018;48:1731–1737.
16. Gabbay V, Bradley KA, Mao X, Ostrover R, Kang G, Shungu DC. Anterior cingulate cortex γ-aminobutyric acid deficits in youth with depression. Transl Psychiatry. 2017;7:e1216.
17. Tkác I, Starcuk Z, Choi IY, Gruetter R. In vivo 1H NMR spectroscopy of rat brain at 1 ms echo time. Magn Reson Med. 1999;41:649–656.
18. Gruetter R. Automatic, localized in vivo adjustment of all first- and second-order shim coils. Magn Reson Med. 1993;29:804–811.
19. Provencher SW. Estimation of metabolite concentrations from localized in vivo proton NMR spectra. Magn Reson Med. 1993;30:672–679.
20. Diener C, Kuehner C, Brusniak W, Ubl B, Wessa M, Flor H. A meta-analysis of neurofunctional imaging studies of emotion and cognition in major depression. NeuroImage. 2012;61:677–685.
21. Du M-Y, Wu Q-Z, Yue Q, Li J, Liao Y, Kuang W-H, et al. Voxelwise meta-analysis of gray matter reduction in major depressive disorder. Prog Neuropsychopharmacol Biol Psychiatry. 2012;36:11–16.

22. Zhang W-N, Chang S-H, Guo L-Y, Zhang K-L, Wang J. The neural correlates of reward-related processing in major depressive disorder: A meta-analysis of functional magnetic resonance imaging studies. J Affect Disord. 2013;151:531–539.
23. Radua J, Borgwardt S, Crescini A, Mataix-Cols D, Meyer-Lindenberg A, McGuire PK, et al. Multimodal meta-analysis of structural and functional brain changes in first episode psychosis and the effects of antipsychotic medication. Neurosci Biobehav Rev. 2012;36:2325–2333.
24. Ramsay IS. An activation likelihood estimate meta-analysis of thalamocortical dysconnectivity in psychosis. Biol Psychiatry Cogn Neurosci Neuroimaging. 2019;4:859–869.
25. Chen P, Ye E, Jin X, Zhu Y, Wang L. Association between thalamocortical functional connectivity abnormalities and cognitive deficits in schizophrenia. Sci Rep. 2019;9:2952.
26. Marsman A, Mandl RC, Klomp DW, Bohlken MM, Boer VO, Andreychenko A, et al. GABA and glutamate in schizophrenia: A 7 T 1H-MRS study. NeuroImage Clin. 2014;6:398–407.
27. Overbeek G, Gawne TJ, Reid MA, Salibi N, Kraguljac NV, White DM, et al. Relationship between cortical excitation and inhibition and task-induced activation and deactivation: A combined magnetic resonance spectroscopy and functional magnetic resonance imaging sudy at 7T in first-episode psychosis. Biol Psychiatry Cogn Neurosci Neuroimaging. 2019;4:121–130.
28. Posporelis S, Coughlin JM, Marsman A, Pradhan S, Tanaka T, Wang H, et al. Decoupling of brain temperature and glutamate in recent onset of schizophrenia: a 7T proton magnetic resonance spectroscopy study. Biol Psychiatry Cogn Neurosci Neuroimaging. 2018;3:248–254.
29. Reid MA, Salibi N, White DM, Gawne TJ, Denney TS, Lahti AC. 7T proton magnetic resonance spectroscopy of the anterior cingulate cortex in first-episode schizophrenia. Schizophr Bull. 2019;45:180–189.
30. Thakkar KN, Rösler L, Wijnen JP, Boer VO, Klomp DW, Cahn W, et al. 7T proton magnetic resonance spectroscopy of gamma-aminobutyric acid, glutamate, and glutamine reveals altered concentrations in patients with schizophrenia and healthy siblings. Biol Psychiatry. 2017;81:525–535.
31. Brandt AS, Unschuld PG, Pradhan S, Lim IAL, Churchill G, Harris AD, et al. Age-related changes in anterior cingulate cortex glutamate in schizophrenia: a 1H MRS Study at 7 Tesla. Schizophr Res. 2016;172:101–105.
32. Taylor R, Neufeld RWJ, Schaefer B, Densmore M, Rajakumar N, Osuch EA, et al. Functional magnetic resonance spectroscopy of glutamate in schizophrenia and major depressive disorder: anterior cingulate activity during a color-word Stroop task. Npj Schizophr. 2015;1:1–8.
33. Taylor R, Osuch EA, Schaefer B, Rajakumar N, Neufeld RWJ, Théberge J, et al. Neurometabolic abnormalities in schizophrenia and depression observed with magnetic resonance spectroscopy at 7 T. BJPsych Open. 2017;3:6–11.
34. Rowland LM, Pradhan S, Korenic S, Wijtenburg SA, Hong LE, Edden RA, et al. Elevated brain lactate in schizophrenia: a 7 T magnetic resonance spectroscopy study. Transl Psychiatry. 2016;6:e967.
35. Kumar J, Liddle EB, Fernandes CC, Palaniyappan L, Hall EL, Robson SE, et al. Glutathione and glutamate in schizophrenia: a 7T MRS study. Mol Psychiatry. 2020;25:873–882.
36. Wang AM, Pradhan S, Coughlin JM, Trivedi A, DuBois SL, Crawford JL, et al. Assessing brain metabolism with 7-T proton magnetic resonance spectroscopy in patients with first-episode psychosis. JAMA Psychiatry. 2019;76:314–323.
37. Li Y, Jakary A, Gillung E, Eisendrath S, Nelson SJ, Mukherjee P, et al. Evaluating metabolites in patients with major depressive disorder who received mindfulness-based cognitive therapy and healthy controls using short echo MRSI at 7 Tesla. Magn Reson Mater Phys Biol Med. 2016;29:523–533.
38. Sydnor VJ, Roalf DR. A meta-analysis of ultra-high field glutamate, glutamine, GABA and glutathione 1HMRS in psychosis: Implications for studies of psychosis risk. Schizophr Res. 2020; doi: 10.1016/j.schres.2020.06.028.

39. Roalf DR, Nanga RPR, Rupert PE, Hariharan H, Quarmley M, Calkins ME, et al. Glutamate imaging (GluCEST) reveals lower brain GluCEST contrast in patients on the psychosis spectrum. Mol Psychiatry. 2017;22:1298–1305.
40. Moriguchi S, Takamiya A, Noda Y, Horita N, Wada M, Tsugawa S, et al. Glutamatergic neurometabolite levels in major depressive disorder: a systematic review and meta-analysis of proton magnetic resonance spectroscopy studies. Mol Psychiatry. 2019:24:952–964.
41. Merritt K, Egerton A, Kempton MJ, Taylor MJ, McGuire PK. Nature of glutamate alterations in schizophrenia: A meta-analysis of proton magnetic resonance spectroscopy studies. JAMA Psychiatry. 2016;73:665–674.
42. Satterthwaite TD, Feczko E, Kaczkurkin AN, Fair DA. Parsing psychiatric heterogeneity through common and unique circuit-level deficits. Biol Psychiatry. 2020;88:4–5.